PROCEEDINGS B

royalsocietypublishing.org/journal/rspb

Research

**Cite this article:** Wong JY, Chan BKK, Chan KYK. 2020 Swimming kinematics and hydrodynamics of barnacle larvae throughout development. *Proc. R. Soc. B* **287**: 20201360. http://dx.doi.org/10.1098/rspb.2020.1360

Received: 10 June 2020
Accepted: 21 September 2020

**Subject Category:**
Morphology and biomechanics

**Subject Areas:**
biomechanics, ecology

**Keywords:**
nauplius, cyprid, flow structure, high-speed imaging, metamorphosis

**Authors for correspondence:**
Benny K. K. Chan
e-mail: chankk@gate.sinica.edu.tw
K. Y. Karen Chan
e-mail: kchan1@swarthmore.edu

Electronic supplementary material is available online at https://doi.org/10.6084/m9.figshare.c.5136225.

THE ROYAL SOCIETY PUBLISHING

# Swimming kinematics and hydrodynamics of barnacle larvae throughout development

J. Y. Wong[1,2,3], Benny K. K. Chan[3] and K. Y. Karen Chan[4]

[1]Department of Life Science, National Taiwan Normal University, Taipei 11677, Taiwan
[2]Biodiversity Program, Taiwan International Graduate Program, Academia Sinica, Taipei 11529, Taiwan
[3]Biodiversity Research Center, Academia Sinica, Taipei 11529, Taiwan
[4]Biology Department, Swarthmore College, Swarthmore, PA 19081, USA

JYW, 0000-0002-8705-0283; BKKC, 0000-0001-9479-024X; KYKC, 0000-0002-7775-4383

Changes in size strongly influence organisms' ecological performances. For aquatic organisms, they can transition from viscosity- to inertia-dominated fluid regimes as they grow. Such transitions are often associated with changes in morphology, swimming speed and kinematics. Barnacles do not fit into this norm as they have two morphologically distinct planktonic larval phases that swim differently but are of comparable sizes and operate in the same fluid regime (Reynolds number $10^0$–$10^1$). We quantified the hydrodynamics of the rocky intertidal stalked barnacle *Capitulum mitella* from the nauplius II to cyprid stage and examined how kinematics and size increases affect its swimming performance. Cyprids beat their appendages in a metachronal wave to swim faster, more smoothly, and with less backwards slip per beat cycle than did all naupliar stages. Micro-particle image velocimetry showed that cyprids generated trailing viscous vortex rings that pushed water backwards for propulsion, contrary to the nauplii's forward suction current for particle capture. Our observations highlight that zooplankton swimming performance can shift via morphological and kinematic modifications without a significant size increase. The divergence in ecological functions through ontogeny in barnacles and the removal of feeding requirement likely contributed to the evolution of the specialized, taxonomically unique cyprid phase.

## 1. Introduction

Organisms typically increase in size and often change morphology through development. These morphological changes are in turn constrained by not only phylogenetics and physiology, but also biomechanics [1–4]. In the aquatic realm, changes in size determine the fluid regimes in which the organisms operate. As small (less than 1 mm) aquatic organisms increase in size, the relative influence of viscous drag diminishes and individuals operate in an increasingly turbulent and inertia-dominated regime. Such a shift in the fluid regime has been associated with increases in swimming and feeding performance [5–7]. However, drastic changes in morphology can also occur without significant size change [8]. To date, few studies have quantified or examined the mechanisms that determine changes in swimming and feeding performance when organisms change shape without a complementary change in fluid regime (but see [9]).

Crustaceans with complex life histories provide a good model system to investigate this relationship between form and function through ontogeny. For holoplanktonic crustaceans such as copepods and *Artemia*, their relatively small larvae (less than 1 mm) operate in an intermediate Reynolds number fluid regime ($Re = 1$–$100$), in which viscosity leads to tradeoffs between maximizing feeding and swimming performance. Size (and thus $Re$) increase generally leads to performance improvement. This improvement can be achieved either by directly elevating the performance of an existing, underperforming larval morphology [5], or by permitting larvae to exploit a different morphology or kinematic mechanism

that are more efficient in higher-*Re* regimes [6]. Often, in crustaceans, the two strategies are inseparable as size increase and morphological change co-occur [10]. However, for barnacles, a crustacean with a biphasic life history—sessile adults and planktonic larvae—their two distinctive planktonic forms, nauplius and cyprid, do not significantly differ in size. And yet, barnacle cyprids swim at significantly higher speeds than the early naupliar stages [11,12]. These observations suggest that performance gains through changes in morphology and/or kinematics are possible without a size increase.

The barnacle life cycle generally consists of six nauplius stages and ends with one cyprid stage. Nauplii swim and feed (except those that are lecithotrophic), and this stage is the primary dispersal phase. All barnacle cyprids are non-feeding; they use a pair of modified antennules for walking, exploring and attaching to substrates for settlement [13]. Metamorphosis from nauplius to cyprid involves profound changes in the overall body form and locomotory appendages. The cyprid is enclosed by a fusiform, bivalved carapace without the projecting structures (e.g. frontal horns and tail spines) seen in the nauplius. Nauplii swim with three pairs of cephalic appendages while cyprids swim with six pairs of thoracic appendages.

Differences in swimming behaviours between nauplii and cyprids, in particular the increase in swimming speed with age, lead to differences in vertical distributions, and hence, cross-shore transport [14,15]. The negative rheotaxis exhibited by cyprids also plays an essential role in attaching to substrates [16]. However, before attachment can take place, initial contact with the substrate is needed, and active swimming against the flow could help increase the settling window [17–19]. Cyprids, therefore, need to meet strong swimming requirements. Indeed, recent observations of tethered barnacle cyprids of *Balanus glandula* highlighted specializations for swimming: the radial movement of the cyprid's thoracopods during the power stroke and the fused setules between these appendages [20]. While tethering allows for an excellent view of appendage movement, it prevents one from making a direct link between swimming kinematics to change in swimming performance and may introduce hydrodynamics artefacts [21,22].

Here, we compare the swimming performances, kinematics and hydrodynamics of freely swimming barnacle larvae across their development from nauplius to cyprid. Larvae of the intertidal rocky shore stalked barnacle, *Capitulum mitella* Linnaeus, 1758, increase in size through the naupliar stages, but do not change size when metamorphosing into cyprids, which represents a typical barnacle's ontogenetic profile. To compare swimming performances, we quantified the displacement gained per beat cycle of free-swimming larvae. We examined whether swimming differences can be attributed to changes in limb location and orientation, body size and/or kinematics of the limb beat. Finally, we compared flow structures around swimming larvae using micro-particle image velocimetry (μPIV) and examined flow characteristics such as trailing vortices and spatial flow decay.

## 2. Methods

### (a) Larval collection and rearing

*Capitulum mitella* adults were collected from rock crevices in Clear Water Bay, Hong Kong (22°20′22″ N, 114°16′ E). Egg masses were dissected from the mantle cavity of the barnacles and maintained in aerated filtered seawater (0.45 μm, 25°C, 33 psu) until the nauplii hatched. Hatched nauplii were collected with a pointed light source and transferred to fresh filtered seawater. Nauplii were fed with a mixture of *Isochrysis galbana* and *Tetraselmis chuii ad libitum* until they moulted into stage VI. For stage VI nauplii, *Rhodomonas salina* was used in place of *T. chuii* until nauplii moulted into the cyprid stage. Individuals were fed and their seawater was changed daily. Nauplii II to VI were filmed on the 1st, 2nd, 4th, 5th and 7th day after hatching, respectively. We did not obtain video of nauplius I, which moulted into nauplius II within hours on the first day. Metamorphosis into cyprids first occurred on the 12th day of rearing, and 2-day-old cyprids were used for video observations. Morphometrics data of nauplii and cyprids were measured from video frames with ImageJ (electronic supplementary material, table S1).

### (b) Video acquisition

Videos of free-swimming nauplii and cyprids were taken with a high-speed camera (FastCam Mini UX100, Photron Ltd.) at 2000 frames $s^{-1}$ and a final resolution of 1280 × 1024 pixels. Magnification was achieved with an extended focal distance created with a bellows and a Nikon 60 mm F2.8 lens. Videos had fields of view of 2.0 × 1.6 mm to 2.9 × 2.3 mm and estimated focal depths of approximately 20–30 μm (see electronic supplementary material). This high-speed microscale imaging system was modelled after the ones described in [23,24]. About 30 nauplius or cyprid individuals were recorded in each video session inside a custom-made cuvette (25 × 75 × 5 mm) illuminated by an array of white LEDs. Recordings were taken inside a temperature-controlled room at 25°C, and an external 400 ml water bath was used to house the recording chamber to further buffer small temperature fluctuations. Microalgae (*Isochrysis galbana*) were used as seeding particles to trace fluid around nauplii and cyprid, except stage II nauplius for which neutrally buoyant micro-plastics beads (5 μm in diameter, Spherotech Inc.) were used. Five videos were analysed for each stage (electronic supplementary material, table S1).

### (c) Swimming characterization

To compare swimming performances, we calculated swimming velocity based on the displacement of the naupliar or cyprid body centroids over time. One beat cycle was analysed for each individual as most individuals only stayed in the plane of focus for fewer than two beat cycles. The 'relative swimming speed' was also calculated by normalizing absolute swimming speed against larval length. Forward displacement was defined as a displacement vector that has a positive dot product with the body's direction vector (i.e. a vector from the body's posterior end to the anterior end, and vice versa for backwards displacement). To compare the efficiency of propulsion, we calculated the forward to backwards displacement ratio. Net displacement over a beat cycle (see details in the kinematics analysis), both absolute and normalized by larval length, was also calculated. To determine the flow regime the larvae swam in, Reynolds number (*Re*) was calculated with the equation [25]

$$Re = \frac{lU}{v}.$$

Characteristic length $l$ is the larval total length and speed $U$ is the mean swimming speed of each individual. The value of kinematic viscosity ($v = 0.934 \times 10^{-6}$ $m^2$ $s^{-1}$) for 33 psu seawater at 25°C was used. Swimming metrics for nauplii (5 for each stage) were calculated from dorsal view videos, but a mix of dorsal and lateral views (3 dorsal : 2 lateral) were used for cyprids due to the difficulty in obtaining videos from the dorsal view.

### (d) Kinematics analysis

To compare the pattern of appendages' movement over a beat cycle, appendage angles were calculated from the tip of the

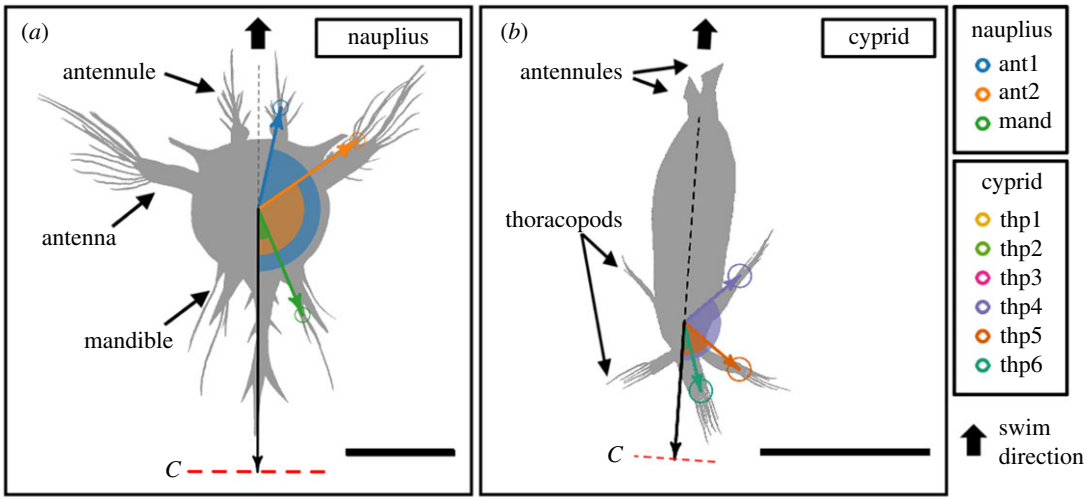


**Figure 1.** Schematics illustrating angle measurements made for nauplius (*a*) and cyprid (*b*). The line *C* (red dash) is used to calculate flux, with length equal to head shield and carapace width for nauplius and cyprids, respectively. Scale bar for both nauplius and cyprids denotes 300 µm. ant1 = antennule; ant2 = antenna; mand = mandible; thp1 to thp6 = thoracopod 1 to 6. Note that not all thoracopods are visible during power stroke from dorsal view (see electronic supplementary material, video S2 for details). (Online version in colour.)

appendage relative to the body axis (figure 1). Only the right side was digitized. From these angles, we calculated stroke amplitude by mapping the range of the angles for each appendage and angular speed by taking time derivatives of the angles.

To examine the consequences of differences in numbers of appendages and timing of the appendage recovery stroke, we calculated the duration of the power stroke ($T_P$) and recovery stroke ($T_R$) over a beat cycle and the $T_P : T_R$ ratio. For nauplii, $T_P$ was estimated from the beginning of the mandible's beat to the end of the antenna's beat, while $T_R$ was from the beginning of the mandible's return to the end of the antenna's return. Under this definition, there was an overlap between the power and recovery strokes, so the sum of $T_P$ and $T_R$ exceeded the duration of one beat cycle of an individual appendage used to calculate frequency. For cyprids, $T_P$ was estimated from the beginning of the 6th thoracopod's beat to the end of the 1st thoracopod's beat, while $T_R$ was from the beginning of the 6th thoracopod's return to the end of the 1st thoracopod's return. We computed three additional dimensionless indices to describe the kinematics of the larval motion. They are: (i) the jump number ($N_{jump}$) that describes the characteristics of the imposed flows [26]; (ii) the Strouhal number ($St$) that characterizes swimming performance in relation to the oscillatory beats [27]; and (iii) the advance ratio ($J$) that compares larval swimming speed to speed of appendage tips [27,28]:

$$N_{jump} = \frac{T_P}{l^2/4v},$$

$$St = \frac{fA}{U} \text{ and}$$

$$J = \frac{U}{2\theta f L m}.$$

$T_P$ is the duration of the power stroke, $l$ is the larval total length, $v$ is the kinematic viscosity, $f$ is the beat frequency, $A$ is the amplitude in distance travelled by appendage, $U$ is the average swimming speed, $\theta$ is the mean appendage amplitude in radian, $L$ is the mean appendage length (including setae) and $m$ is the number of appendage pairs to account for the difference in a number of appendages used for propulsion. $m = 2$ for nauplii because we assumed antennules contribute little towards propulsion; and $m = 5$ for cyprids because the amplitude of the 1st pair of thoracopods could not be measured in our dataset.

## (e) Hydrodynamics analysis

To compare flow structures around swimming nauplii and cyprids through ontogeny, flow was visualized as flow velocity vectors overlaid over a vorticity map. Cross-correlations of video frames were computed to obtained velocity vectors after masking larvae. Cross-correlation was computed with a multi-pass algorithm with interrogation windows decreasing in size from 96 × 96 to 64 × 64 pixels with 50% overlaps. Vector post-processing was performed to remove outlier vectors. To show fluid disturbance caused by the beating of appendages, two-dimensional 'flux' at the posterior end of the larva was computed. Flux for each frame was calculated for flow passing through a line segment equal to the larva's body width at the body's posterior end, centred at the long axis of the larva (figure 1). Body width was chosen for flux computation because it encompasses the distance within the reach of the mandibles, the appendages used to bring food particle to the labrum. Flux was computed by integrating the velocity vector projected onto the normal direction over the line segment. Positive flux indicates fluid flowing in the opposite direction of the body vector and vice versa. To compare predation risk as a hydrodynamic signal presented to predators resulted from the flow disturbance, the power of spatial flow attenuation with respect to distance was calculated following the method presented in [29]. We further characterized the trailing wake vortices of cyprids by examining the separation of velocity stagnation points from vorticity maximum/minimum, a feature of viscous vortex ring [30].

## (f) Software and statistical analysis

Body landmarks and tips of appendages were marked in 'tpsDig2' [31]. Cross-correlation and subsequent computation of vorticity were performed in 'DaVis' software (v. 8.2.1, LaVision GmbH). Swimming, kinematic and hydrodynamic analyses were computed with 'npiv' R package (v. 0.0.1; [32]). The package was slightly modified for cyprids as the original software was intended for nauplii. The modified version is available from the first author upon request. Statistical analyses were performed in R (www.r-project.org). Analysis of variance (ANOVA) was used to compare mean differences between ontogenetic stages, followed by Tukey's HSD test for pairwise comparisons if the difference was significant for the main effect. Data were log-transformed for swimming speed (both absolute and relative) and the forward: backwards displacement ratio before being subjected to ANOVA to

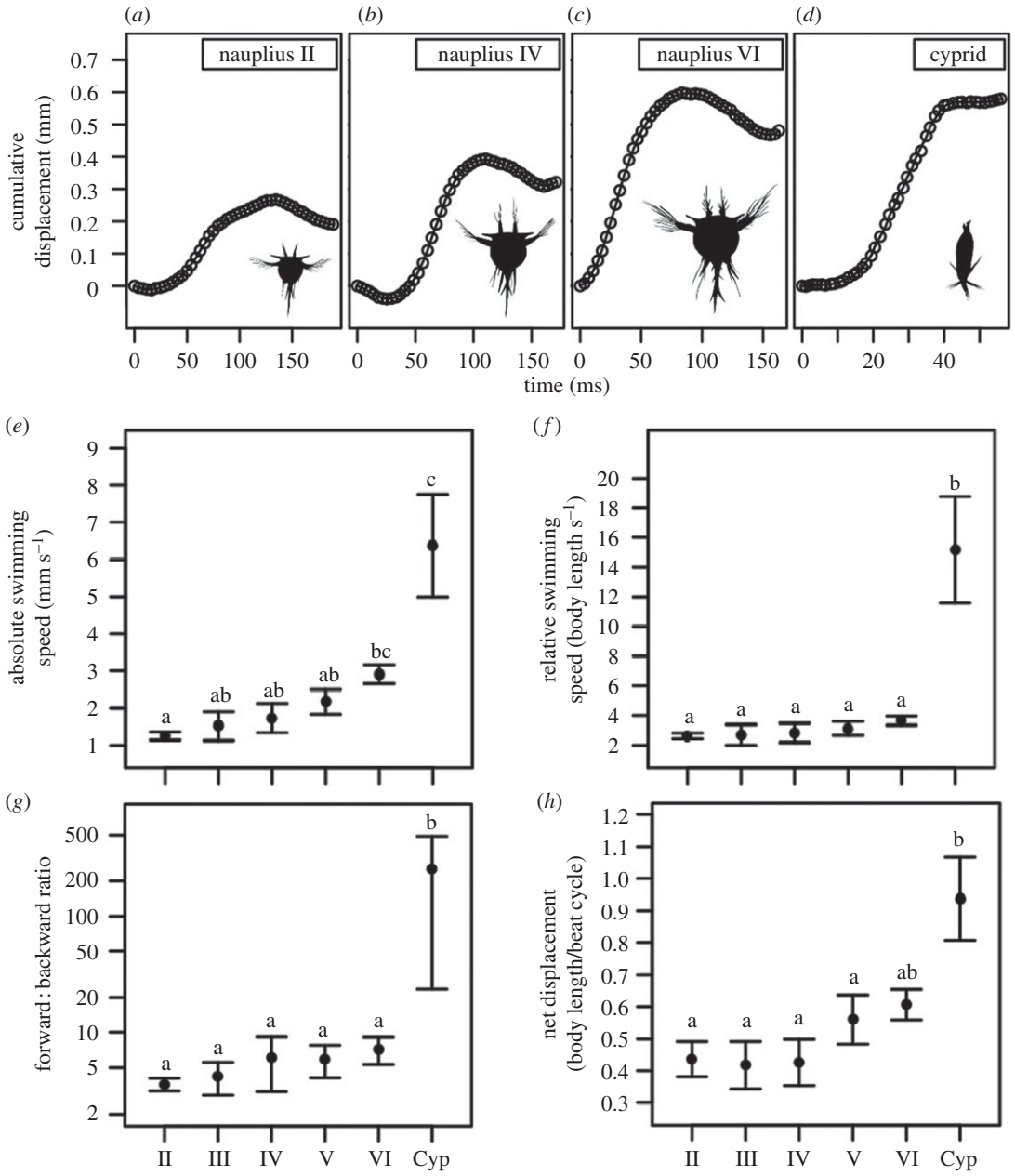


**Figure 2.** Representative profiles of cumulative displacement in nauplii and cyprid (*a–d*). Cyprids had higher absolute and relative swimming speed (*e*,*f*), forward : backwards displacement ratio (*g*) and net displacement per beat cycle (*h*). Note: *y*-axis in (*e*) is on a logarithmic scale. Means ± s.e. are shown ($n = 5$), letters denote grouping from Tukey-adjusted pairwise comparisons. II–VI = naupliar stages II to VI; Cyp = cyprid.

homogenize variance between the ontogenetic stages. The statistical significance level was set to $p < 0.05$.

## 3. Results

### (a) Larval size

Larval total length increased gradually from 476 ± 13 µm in nauplius II to 798 ± 6 µm in nauplius VI (mean ± s.e., table 1). Similarly, larval width increased from 205 ± 5 µm in nauplius II to 351 ± 9 µm in nauplius VI. Instead of a size increase, there was a nearly 50% decrease in larval length and width between nauplius VI and cyprid, with a total length of 429 ± 13 µm and a total width of 141 ± 10 µm for cyprids (mean ± s.e., table 1).

### (b) Swimming speed

Absolute swimming speed increased through ontogeny, from 1.2 ± 0.1 mm $s^{-1}$ in nauplius II to 2.9 ± 0.3 mm $s^{-1}$ in nauplius VI, and it further increased to 6.4 ± 1.4 mm $s^{-1}$ in cyprids (mean ± s.e., figure 2*e*). Between naupliar stages, absolute swimming speed was only significantly different between stages II and VI. Cyprids swam significantly faster than all naupliar stages except for nauplius VI. After normalization by larval length, naupliar relative swimming speed ranged from 2.6 ± 0.2 body length per second (BL $s^{-1}$) in nauplius II to 3.7 ± 0.3 BL $s^{-1}$ in nauplius VI (mean ± s.e.). No significant difference in relative swimming speed was found between naupliar stages. Cyprids swam at 15.2 ± 3.6 BL $s^{-1}$ (i.e. 4 to 6 times faster than any naupliar stages; figure 2*f*).

### (c) Flow regimes

Reynolds number (*Re*) increased gradually through ontogeny but stayed well below 10 (electronic supplementary material, table S1). Nauplius VI had significantly larger *Re* than the two earliest stages (nauplius II and III). Although cyprids had a significantly higher *Re* than stage II to V nauplii, there

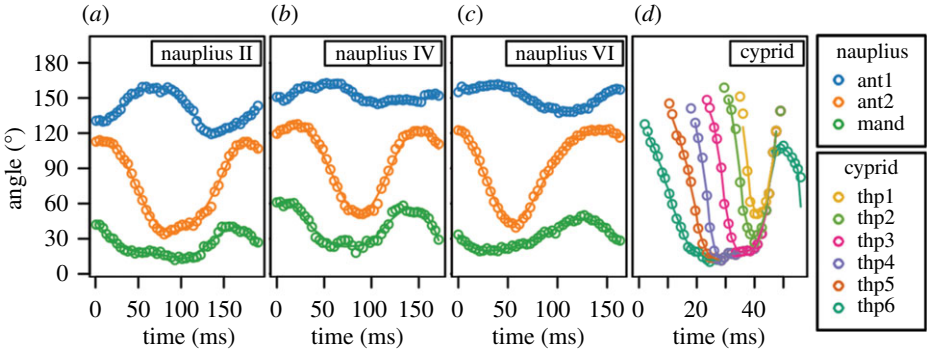


**Figure 3.** Representative profiles of time evolutions for the angular positions of appendages over a beat cycle for nauplius II (*a*), nauplius IV (*b*), nauplius VI (*c*) and cyprid (*d*).

was no significant difference between cyprids and nauplius VI for either *Re* value calculated from characteristic length with and without antennules. The *Re* of nauplius VI increased to 3.4 ± 0.7 (17.7 ± 3.7% increase, same as the increase in larval length) when antennules were included in the calculation.

## (d) Displacement per beat cycle

All nauplii pushed themselves forward during the power stroke and slipped backwards during the recovery stroke, resulting in jerky swimming (figure 2*a–c*; electronic supplementary material, video S1). No significant difference was detected in their forward : backward displacement ratios (figure 2*g*). By contrast, cyprids swam smoothly with very little backwards displacement during the recovery stroke, resulting in a forward: backwards displacement ratio up to an order of magnitude higher in the naupliar stages (figure 2*g*; electronic supplementary material, video S2). Cyprids finished a beat cycle in less time and reached a similar net displacement as nauplius VI at the end, despite being smaller in size (figure 2*d*). Cyprids completed their beat cycles at a higher frequency than any naupliar stages (15.4 ± 1.8 Hz compared with approximately 6 Hz for all nauplii, electronic supplementary material, table S1). Cyprid net displacement per beat cycle was significantly higher than that of nauplius II, but was not significantly different to those of nauplius III to VI. After normalization by larval length, cyprids propelled themselves significantly further per beat cycle than any naupliar stages but nauplius VI ($p$-value = 0.07; figure 2*h*).

## (e) Kinematics

Nauplii swam by paddling their mandibles backwards first, followed by the antennae, and they began to return to the starting position at the end of the antennae's power stroke in a metachronal manner (figure 3*a–c*; electronic supplementary material, video S1). However, the mandibles reached the starting position first and began the power stroke while the antennae were still returning to the starting position. The antennules spent little time moving in the same direction as the antennae and mandibles. The antennae's stroke amplitudes were significantly larger than those of the antennules and mandibles (electronic supplementary material, table S1). This pattern of appendage movement was similar across all naupliar stages, and nauplii of all stages completed their beat cycle in a similar amount of time (i.e. there was no significant difference in beat cycle frequencies across naupliar stages). There was also no significant difference in the appendages' amplitudes across the naupliar stages, except for antennules, for which the amplitudes were significantly higher in nauplius II than nauplius IV.

Cyprids swam by beating first the sixth thoracopods and then the remaining thoracopods pair by pair in a metachronal wave (figure 3*d*; electronic supplementary material, video S2). Thoracopod pairs stayed pointing posteriorly at the end of their respective power strokes until almost all pairs reached the end of the power stroke, at which point they returned to the starting positions together. The first thoracopod pair met the other five returning pairs during its power stroke and returned together with the others. Thus, the first thoracopod pair had a smaller beat amplitude than the other pairs, which all had similar stroke amplitudes (electronic supplementary material, table S1). Contrary to the naupliar beat patterns, the cyprid's metachronal power stroke had similar appendage amplitudes, and all thoracopod pairs moved in sync during the recovery stroke. In addition, the thoracopods beat very rapidly, reaching an average angular speed an order of magnitude higher than that of the nauplii's main propelling appendage, the antennae (electronic supplementary material, table S1). The simultaneous recovery stroke pattern in cyprids also increased the ratio of time spent for the power stroke to time spent for the recovery stroke ($T_P : T_R$). Nauplii had nearly symmetrical durations of power and recovery strokes, which did not differ across stages (electronic supplementary material, table S1). While the Strouhal numbers were higher in nauplii ($St > 1$) than cyprid ($St = 0.74$), stage or larval phase had no statistically significant effect on Strouhal number (electronic supplementary material, table S1). After accounting for the difference in a number of appendage pairs, stage VI nauplii had significantly higher advance ratio ($J$) than cyprids ($p < 0.05$; electronic supplementary material, table S1).

## (f) Topology of flow structure

Swimming nauplii and cyprids generated distinct flow structures around them. During the power stroke, nauplii had vortices around their bodies and cyprids generated counter-rotating vortices in the trailing wake (figure 4*a–j*; electronic supplementary material, videos S3 and S4). With the $N_{jump}$ in the order of 1, the flow fields imposed by both nauplii and cyprids could be characterized as viscous decay. In nauplii, weak vortices were generated only when the nauplii paddled their mandibles, which were more noticeable in nauplius IV to VI (figure 4*a–e*). The vortices formed by the beating

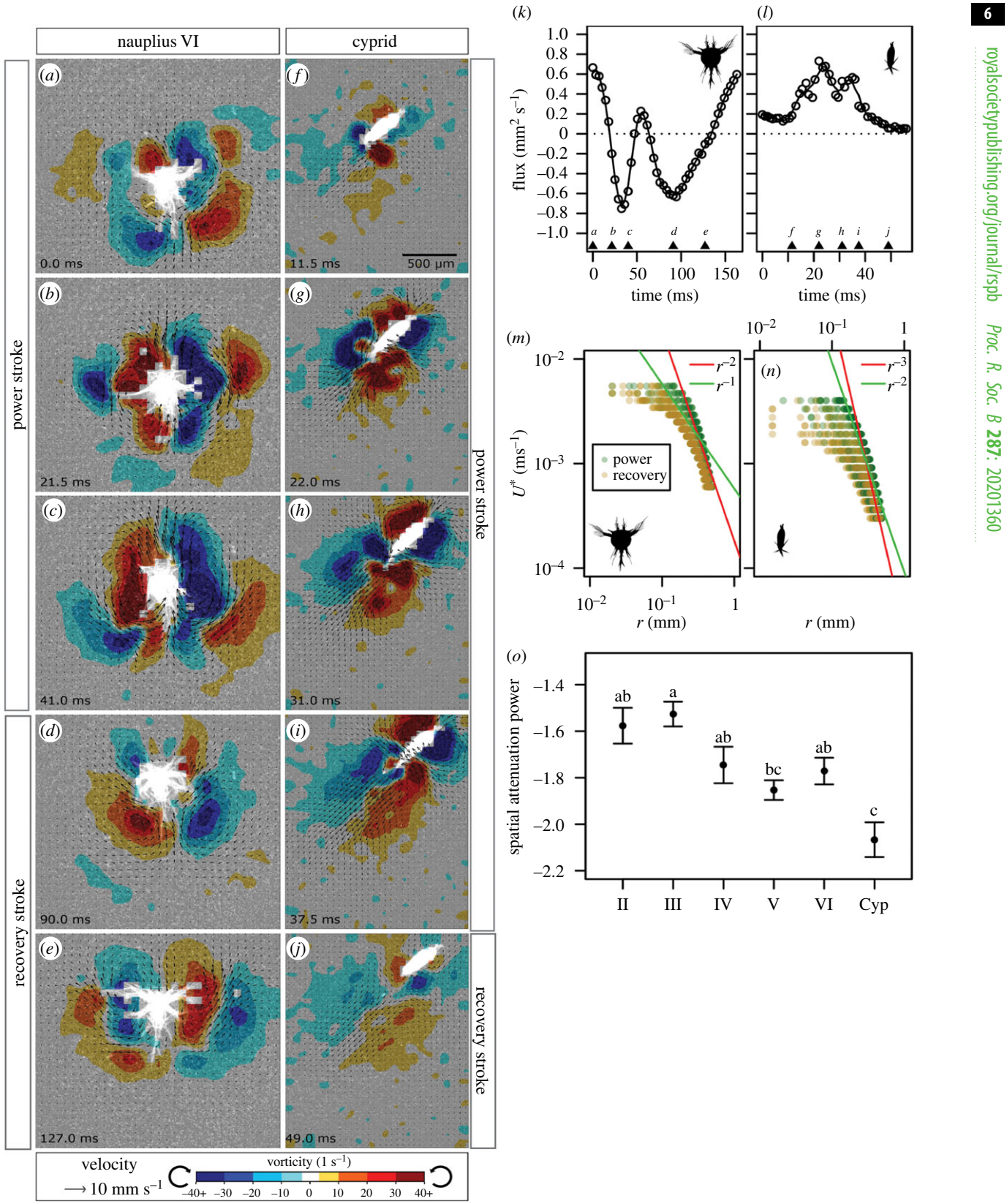


**Figure 4.** Snapshots of vorticity fields overlaid with velocity vectors around a representative swimming nauplius VI and a cyprid from ventral and dorsal view (same individuals in figure 3*c*,*d*, respectively). Absolute flux change over a beat cycle for nauplius VI (*k*) and cyprid (*l*). Positive values indicate flow leaving larva and *vice versa*. Small triangles on time axes of *k*–*n* indicate the time positions of snapshots used in *a*–*j*. (*m*–*n*) Representative profile of *U** plotted against *r*, where *U** is the binned flow speed and *r* is the radius of the circle with equivalent area to the area occupied by *U** in the flow field. Fit lines of attenuation power of theoretical propulsion models are overlaid. power = power stroke; recovery = recovery stroke. (*o*) Empirical power fittings for spatial flow attenuation (mean ± s.e., $n = 5$). Letters denote grouping from Tukey-adjusted pairwise comparisons. II–VI = naupliar stages II to VI; Cyp = cyprid.

mandibles of nauplii dissipated at the end of the mandible's power stroke and was replaced by the vortices formed by the moving antennae, which carried fluid along the moving body. By contrast, the cyprids' wake vortices were reinforced by successive thoracopod beating before they dissipated, effectively extending the peak circulation (electronic supplementary material, video S4). Positive value of the flux at the trailing edge of cyprids confirmed that the vortices moved water away body

(i.e. against the direction of travel; figure 4*k*,*l*). The velocity stagnation points were separated from the vorticity maximum/minimum indicating cyprids generated trailing viscous vortex rings (electronic supplementary material, video S5).

During the recovery stroke, nauplii's returning appendages created vortices with reversed directions (i.e. same as the direction of travel, towards the body) that were smaller in magnitude compared with those generated during the power stroke. By contrast, cyprids returned collapsed thoracopods simultaneously and created much smaller fluid disturbance than that created during the power stroke (figure 4*J*).

### (g) Spatial attenuation of fluid disturbance

During the power stroke, the area disturbed by swimming cyprids was larger than that of nauplii, as indicated by the greater area of influence radius standardized by larval size (electronic supplementary material, table S1). However, the power of flow decay over distance was lower in cyprids than all naupliar stages except nauplius V (figure 4*m–o*), meaning that cyprids generated flow that attenuated faster spatially.

## 4. Discussion

Size increases and the resulting fluid regime changes during development have been linked to improved swimming performance in small aquatic organisms [5,7,33]. Contrary to this pattern, our comparison of the stalked barnacle *Capitulum mitella* larvae across developmental stages shows that cyprids swim faster and smoother than their preceding naupliar stages of similar or larger sizes. In addition to having a more streamlined body and twice the number of appendages than the nauplius, cyprids' higher swimming efficiency could also be explained by differences in kinematics, namely beat frequency, angular velocity and limb synchronicity during the recovery stroke. These kinematics differences were reflected in the presence of trailing viscous vortex rings in the wake of cyprids and their absence around nauplii. These differences are likely linked to their respective ecological roles in the barnacle life cycle: feeding and dispersal in nauplius versus settlement in cyprids. The swimming specialization in cyprids highlights the changing selective pressure exerted on the distinct larval phases.

### (a) Swimming speed increases throughout development

*Capitulum mitella* naupliar swimming speed fits the expectation that higher swimming speed comes with the larger size, but only between the stages with large size differences, i.e. between nauplius II and VI (figure 2*e–f*). Despite being smaller in size (electronic supplementary material, table S1), *C. mitella* cyprids swam faster than almost all preceding naupliar stages of larger sizes, similar to previous findings on other barnacle larvae [12]. However, *C. mitella* cyprids swam considerably slower at 7 mm $s^{-1}$ than the previously reported speeds of 18–95 mm $s^{-1}$ for other species [14,16,18]. Our observations were made in still water, and this setting may have led to an underestimated swimming speed of *C. mitella* cyprids. Cyprids' swimming speeds had been previously shown to be highly variable over distance [34] and can be elevated by downwelling water flow [14]. Regardless of whether the swimming speed of cyprids could be higher in the field, our measurements clearly demonstrated that the shift in swimming speed could have little to do with size.

### (b) Cyprids swam more effectively without increasing *Re*

*Capitulum mitella* nauplii experienced high backwards displacement during the recovery stroke and are therefore inefficient swimmers. This backwards displacement problem is universal to all rowing swimmers in low- to intermediate-*Re* regimes [35]. One solution to this problem is to operate at a higher *Re*, in which inertia dominates, such that the swimmer can glide at the end of the power stroke and reduce backwards displacement [36]. For example, an increased *Re* through ontogeny (from 2 to 37) helped *Artemia* reduce backwards displacement [6]. By contrast, the *Re* of *C. mitella* larvae remained less than 10 throughout development, and we did not observe cyprids gliding into the recovery stroke. Thus, it is possible to swim efficiently and reduce backwards slip without significantly shifting the fluid regime.

Given that both nauplii and cyprids operate in low to intermediate *Re* regimes, reciprocal motion (i.e. symmetry in appendages' configurations between the power and recovery strokes) would result in little net displacement [35]. Reciprocal motion could break in two ways, by changing the effective area that appendages sweep through between the power and recovery strokes, or by having multiple pairs of appendages beat in metachronal wave and return simultaneously [37,38]. Kinematics comparisons show that *Capitulum mitella* cyprids employed both ways to break reciprocal motion. First, cyprids maximized the sweeping area of thoracopods during the power stroke by extending them radially and minimized the sweeping area by collapsing them medially during the return stroke. Second, cyprids beat their thoracopods in a metachronal wave and brought them back together in synchrony (figure 3*d*). By contrast, both the power and recovery strokes of nauplii were metachronal. Cyprids, therefore, achieve large asymmetries in their effective sweeping areas and appendage movements between power and recovery strokes. Such asymmetries in turn confer swimming efficiency.

The lower advance ratio ($J$) in cyprids further supports the direct contribution of higher limb beat frequency and number of legs towards cyprid's faster swimming (electronic supplementary material, table S1). Although increasing the number of appendages help with elevating body speed, it is hard to physically accommodate them without a commensurate size increase [39]. Cyprid has very tightly spaced appendages with the ratio of space between pairs ($B$) to appendage length ($L$) of approximately 0.1, which is smaller than that of larger crustaceans [39,40]. However, this tightly packed limb arrangement is deemed optimal for low to intermediate *Re* metachronal swimmers, a group which cyprids belong [41]. Despite having more tightly packed appendages than the nauplii stage, for which $B/L$ are approximately 0.15, cyprids paddled their appendages with higher amplitudes (electronic supplementary material, table S1). The appendages did not significantly interfere with each other, probably due to the synchronous rather than metachronal recovery stroke [42,43]. There was also a trend of decreasing Strouhal number ($St$), from approximately 1 in nauplii to less than 1 in cyprids, though statistically insignificant (electronic supplementary material, table S1). For swimming and flying animals operating at high Reynolds number ($Re > 10^2$), including copepod adults [44], $St$ often fell

within the range of 0.2–0.4, which also coincides with the peak propulsion efficiency [45]. Neither nauplii nor cyprids swim with *St* within this narrow range, but the observed *St* values were comparable to those found for pelagic copepod's naupliar and copepodid larvae [10]. This comparison of dimensionless numbers highlights that increased in swimming speed without an overall size increase at low *Re* is achievable but require both morphological and kinematic optimization.

The observed differences in kinematics translated into differences in fluid disturbance patterns between nauplius and cyprid stages (figure 4). Three major differences were observed. First, the area of influence was significantly smaller during the recovery stroke than the power stroke in cyprids, reinforcing the notion that they are efficient in reducing backwards motion. Second, cyprids generate trailing wake vortices that were absent in nauplii. Third, we found a significant reduction in the power of spatial flow attenuation between most naupliar and cyprid stages [29]. By computing the jump number ($N_{jump}$) and observing the separation of velocity stagnation points from the vorticity maximum/minimum (electronic supplementary material, video S5), the flow disturbance observed for both nauplii and cyprids agree with the features of viscous vortex rings ($N_{jump} \sim 1$). Contrary to momentum jets, viscous vortex rings are intermittent in nature and represent a stealthy way of swimming [3,23,26]. It is noteworthy that the major distinctions in dominant flow structures between nauplii and cyprids remained robust across the whole range of *Re* observed. In other words, the flow field around the nauplius with highest *Re* observed was still significantly different from that of the cyprid with the lowest *Re* of the group (electronic supplementary material, figures S1 and S2, and videos S6 and S7). The flow structure distinctions that we observed are very similar to those found between nauplius and copepodids for pelagic copepods, which are explained by changes in both size and morphology [10].

### (c) Distinct habitat requirements shape swimming patterns

The differences in kinematics, hydrodynamics and swimming performance between nauplii and cyprids reflect the different ecological roles of these two larval phases. *Capitulum mitella* nauplii swim and feed at the same time, but cyprids are non-feeding and swim to locate attachment sites. Planktotrophic barnacle nauplii's feeding relies on the suction current generated during the recovery stroke [46]. Having a relatively longer duration of recovery stroke generates flows of larger magnitude and area and thus contributes towards particle capture in nauplii. With swimming and feeding integrated, the trade-offs between these two functions could impose a constraint on swimming performance among nauplii, as seen in the comparison between planktotrophic and lecithotrophic nauplii [32]. By contrast, cyprids' swimming appendages are not involved in feeding, nor substrate walking or adhesion.

Swimming specialization in cyprids probably helps larvae navigate complex and turbulent flows near settlement sites [18]. Our data suggest that the evolution of a distinct cyprid form was not likely driven by an ontogenetic niche shift resulting from size increases similar to those proposed for holoplanktonic copepods [47]. Instead, the shift in swimming performance from nauplius to cyprid was achieved through morphological and kinematic changes and reflects a change in the contrasting ecological demands of living in the plankton and swimming towards settlement surfaces.

Ethics. This study does not present research with ethical considerations.

Data accessibility. Data to reproduce the results are deposited in Open Science Framework: https://osf.io/h6jp9/.

Author contributions. J.Y.W. collected the data and carried out the analysis. All authors conceived and designed the study, drafted the manuscript and gave approval for publication.

Competing interests. We declare we have no competing interests.

Funding. Funding of this project is provided by the Ministry of Science and Technology, Taiwan (106-2923-B-001-002-MY3) and Academia Sinica Senior Investigator Award (AS-IA-105-L03) to B.K.K.C. and the Croucher Foundation to K.Y.K.C. J.Y.W. is supported by a TIGP PhD Fellowship.

Acknowledgements. We thank P.-C. Tsai, J. Ngo and D. Tong for their technical assistance. We also acknowledge the language editing service provided by Third Draft Editing. We thank the two anonymous reviewers for their insightful comments.

## References

1. Holzman R, Collar DC, Price SA, Hulsey CD, Thomson RC, Wainwright PC. 2012 Biomechanical trade-offs bias rates of evolution in the feeding apparatus of fishes. *Proc. R. Soc. B* **279**, 1287–1292. (doi:10.1098/rspb.2011.1838)
2. West GB, Brown JH, Enquist BJ. 1997 A general model for the origin of allometric scaling laws in biology. *Science* **276**, 122. (doi:10.1126/science.276.5309.122)
3. Katija K, Colin SP, Costello JH, Jiang H. 2015 Ontogenetic propulsive transitions by *Sarsia tubulosa* medusae. *J. Exp. Biol.* **218**, 2333–2343. (doi:10.1242/jeb.115832)
4. Koehl MAR. 1999 Ecological biomechanics of benthic organisms: life history, mechanical design and temporal patterns of mechanical stress. *J. Exp. Biol.* **202**, 3469–3476.
5. China V, Holzman R. 2014 Hydrodynamic starvation in first-feeding larval fishes. *Proc. Natl Acad. Sci. USA* **111**, 8083–8088. (doi:10.1073/pnas.1323205111)
6. Williams TA. 1994 A model of rowing propulsion and the ontogeny of locomotion in *Artemia* larvae. *Biol. Bull.* **187**, 164–173. (doi:doi:10.2307/1542239)
7. Nagata RM, Morandini AC, Colin SP, Migotto AE, Costello JH. 2016 Transitions in morphologies, fluid regimes, and feeding mechanisms during development of the medusa *Lychnorhiza lucerna*. *Mar. Ecol. Prog. Ser.* **557**, 145–159. (doi:10.3354/meps11855)
8. Strathmann RR. 2018 Larvae and direct development. In *Life histories* (ed. GWM Thiel), pp. 151–177. New York, NY: Oxford University Press.
9. Jiang H, Paffenhöfer GA. 2020 Vortical feeding currents in nauplii of the calanoid copepod *Eucalanus pileatus*. *Mar. Ecol. Prog. Ser.* **638**, 51–63. (doi:10.3354/meps13250)
10. Wadhwa N, Andersen A, Kiorboe T. 2014 Hydrodynamics and energetics of jumping copepod nauplii and copepodids. *J. Exp. Biol.* **217**, 3085–3094. (doi:10.1242/jeb.105676)
11. Sorochan KA, Metaxas A. 2017 The effect of temperature on motility of the nauplius and cypris stages of the acorn barnacle *Semibalanus balanoides*. *Mar. Ecol. Prog. Ser.* **579**, 55–66. (doi:10.3354/meps12246)
12. Walker G. 2004 Swimming speeds of the larval stages of the parasitic barnacle, *Heterosaccus lunatus* (Crustacea: Cirripedia: Rhizocephala). *J. Mar.*

*Biol. Assoc. UK* **84**, 737–742. (doi:10.1017/S002531540400983Xh)
13. Lagersson N, Høeg J. 2002 Settlement behavior and antennulary biomechanics in cypris larvae of *Balanus amphitrite* (Crustacea: Thecostraca: Cirripedia). *Mar. Biol.* **141**, 513–526. (doi:10.1007/s00227-002-0854-1)
14. DiBacco C, Fuchs HL, Pineda J, Helfrich K. 2011 Swimming behavior and velocities of barnacle cyprids in a downwelling flume. *Mar. Ecol. Prog. Ser.* **433**, 131–148. (doi:10.3354/meps09186)
15. Hagerty ML, Reyns N, Pineda J. 2018 Constrained nearshore larval distributions and thermal stratification. *Mar. Ecol. Prog. Ser.* **595**, 105–122. (doi:10.3354/meps12561)
16. Crisp DJ. 1955 The behaviour of barnacle cyprids in relation to water movement over a surface. *J. Exp. Biol.* **32**, 569.
17. Abelson A, Denny M. 1997 Settlement of marine organisms in flow. *Annu. Rev. Ecol. Syst.* **28**, 317–339. (doi:10.1146/annurev.ecolsys.28.1.317)
18. Larsson AI, Granhag LM, Jonsson PR. 2016 Instantaneous flow structures and opportunities for larval settlement: barnacle larvae swim to settle. *PLoS ONE* **11**, e0158957. (doi:10.1371/journal.pone.0158957)
19. Reidenbach MA, Koseff JR, Koehl MAR. 2009 Hydrodynamic forces on larvae affect their settlement on coral reefs in turbulent, wave-driven flow. *Limnol. Oceanogr.* **54**, 318–330. (doi:10.4319/lo.2009.54.1.0318)
20. Lamont EI, Emlet RB. 2018 Permanently fused setules create unusual folding fans used for swimming in cyprid larvae of barnacles. *Biol. Bull.* **235**, 185–194. (doi:10.1086/700084)
21. Emlet RB. 1990 Flow fields around ciliated larvae: effects of natural and artificial tethers. *Mar. Ecol. Prog. Ser.* **63**, 211–225. (doi:10.3354/meps063211)
22. Catton KB, Webster DR, Brown J, Yen J. 2007 Quantitative analysis of tethered and free-swimming copepodid flow fields. *J. Exp. Biol.* **210**, 299–310. (doi:10.1242/jeb.02633)
23. Gemmell BJ, Jiang H, Buskey EJ. 2014 A new approach to micro-scale particle image velocimetry (μPIV) for quantifying flows around free-swimming zooplankton. *J. Plankton Res.* **36**, 1396–1401. (doi:10.1093/plankt/fbu067)
24. Chan KYK, Jiang H, Padilla DK, Humphries S. 2013 Swimming speed of larval snail does not correlate with size and ciliary beat frequency. *PLoS ONE* **8**, e82764. (doi:10.1371/journal.pone.0082764)
25. Vogel S. 1994 *Life in moving fluids*, 2nd edn. Princeton, NJ: Princeton University Press.
26. Jiang H, Kiørboe T. 2011 The fluid dynamics of swimming by jumping in copepods. *J. R Soc. Interface* **8**, 1090–1103. (doi:10.1098/rsif.2010.0481)
27. Murphy DW, Webster DR, Yen J. 2013 The hydrodynamics of hovering in Antarctic krill. *Limnol. Oceanogr. Fluids Environ.* **3**, 240–255. (doi:10.1215/21573689-2401713)
28. Williams TA. 1994 Locomotion in developing *Artemia* larvae: mechanical analysis of antennal propulsors based on large-scale physical models. *Biol. Bull.* **187**, 156–163. (doi:doi:10.2307/1542238)
29. Kiorboe T, Jiang H, Goncalves RJ, Nielsen LT, Wadhwa N. 2014 Flow disturbances generated by feeding and swimming zooplankton. *Proc. Natl Acad. Sci. USA* **111**, 11 738–11 743. (doi:10.1073/pnas.1405260111 M4 - Citavi)
30. Katija K, Jiang H. 2013 Swimming by medusae *Sarsia tubulosa* in the viscous vortex ring limit. *Limnol. Oceanogr. Fluids Environ.* **3**, 103–118. (doi:10.1215/21573689-2338313)
31. Rofhl FJ. 2001 *Thin plate spline digitize (version 2.16)*. New York, NY: Stony Brook University.
32. Wong JY, Chan BKK, Chan KYK. 2020 Evolution of feeding shapes swimming kinematics of barnacle naupliar larvae: a comparison between trophic modes. *Integr. Organ Biol.* **2**, e47486. (doi:10.1093/iob/obaa011)
33. Andersen KH *et al.* 2016 Characteristic sizes of life in the oceans, from bacteria to whales. *Annu. Rev. Mar. Sci.* **8**, 217–241. (doi:10.1146/annurev-marine-122414-034144)
34. Maleschlijski S, Bauer S, Aldred N, Clare AS, Rosenhahn A. 2015 Classification of the pre-settlement behaviour of barnacle cyprids. *J. R Soc. Interface* **12**, 20141104. (doi:10.1098/rsif.2014.1104)
35. Purcell EM. 1977 Life at low Reynolds number. *Am. J. Phys.* **45**, 3–11. (doi:10.1119/1.10903)
36. Williams TA. 1994 The nauplius larva of crustaceans: functional diversity and the phylotypic stage. *Am. Zool.* **34**, 562–569. (doi:10.1093/icb/34.4.562)
37. Lenz PH, Takagi D, Hartline DK. 2015 Choreographed swimming of copepod nauplii. *J. R Soc. Interface* **12**, 20150776. (doi:10.1098/rsif.2015.0776)
38. Takagi D. 2015 Swimming with stiff legs at low Reynolds number. *Phys. Rev. E* **92**, 023020. (doi:10.1103/PhysRevE.92.023020)
39. Murphy DW, Webster DR, Kawaguchi S, King R, Yen J. 2011 Metachronal swimming in Antarctic krill: gait kinematics and system design. *Mar. Biol.* **158**, 2541–2554. (doi:10.1007/s00227-011-1755-y)
40. Campos EO, Vilhena D, Caldwell RL. 2012 Pleopod rowing Is used to achieve high forward swimming speeds during the escape response of *Odontodactylus havanensis* (Stomatopoda). *J. Crust. Biol.* **32**, 171–179. (doi:10.1163/193724011X615596)
41. Granzier-Nakajima S, Guy RD, Zhang-Molina C. 2020 A numerical study of metachronal propulsion at low to intermediate Reynolds numbers. *Fluids* **5**, 86. (doi:10.3390/fluids5020086)
42. Zhang C, Guy RD, Mulloney B, Zhang Q, Lewis TJ. 2014 Neural mechanism of optimal limb coordination in crustacean swimming. *Proc. Natl Acad. Sci. USA* **111**, 13 840–13 845. (doi:10.1073/pnas.1323208111)
43. Ford MP, Lai HK, Samaee M, Santhanakrishnan A. 2019 Hydrodynamics of metachronal paddling: effects of varying Reynolds number and phase lag. *R. Soc. Open Sci.* **6**, 191387. (doi:10.1098/rsos.191387)
44. Kiørboe T, Andersen A, Langlois VJ, Jakobsen HH. 2010 Unsteady motion: escape jumps in planktonic copepods, their kinematics and energetics. *J. R Soc. Interface* **7**, 1591–1602. (doi:10.1098/rsif.2010.0176)
45. Taylor GK, Nudds RL, Thomas ALR. 2003 Flying and swimming animals cruise at a Strouhal number tuned for high power efficiency. *Nature* **425**, 707–711. (doi:10.1038/nature02000)
46. Lochhead JH. 1936 On the feeding mechanism of the nauplius of *Balanus perforatus* Bruguière. *Zool. J. Linn. Soc.* **39**, 429–442. (doi:10.1111/j.1096-3642.1936.tb00477.x)
47. Werner EE. 1988 Size, scaling, and the evolution of complex life cycles. In *Size-structured populations* (eds B Ebenman, L Persson), pp. 60–81. Berlin, Germany: Springer.